Article

Mechanosensitivity of a Rapid Bioluminescence Reporter System Assessed by Atomic Force Microscopy

Benoit Tesson[1,*] and Michael I. Latz[1,*]
[1]Scripps Institution of Oceanography, University of California San Diego, La Jolla, California

ABSTRACT Cells are sophisticated integrators of mechanical stimuli that lead to physiological, biochemical, and genetic responses. The bioluminescence of dinoflagellates, alveolate protists that use light emission for predator defense, serves as a rapid noninvasive whole-cell reporter of mechanosensitivity. In this study, we used atomic force microscopy (AFM) to explore the relationship between cell mechanical properties and mechanosensitivity in live cells of the dinoflagellate *Pyrocystis lunula*. Cell stiffness was 0.56 MPa, consistent with cells possessing a cell wall. Cell response depended on both the magnitude and velocity of the applied force. At the maximum stimulation velocity of 390 μm s^{-1}, the threshold response occurred at a force of 7.2 μN, resulting in a contact time of 6.1 ms and indentation of 2.1 μm. Cells did not respond to a low stimulation velocity of 20 μm s^{-1}, indicating a velocity dependent response that, based on stress relaxation experiments, was explained by the cell viscoelastic properties. This study demonstrates the use of AFM to study mechanosensitivity in a cell system that responds at fast timescales, and provides insights into how viscoelastic properties affect mechanosensitivity. It also provides a comparison with previous studies using hydrodynamic stimulation, showing the discrepancy in cell response between direct compressive forces using AFM and those within flow fields based on average flow properties.

INTRODUCTION

All organisms experience mechanical stress because of gravity, tensile forces, compressive forces, hydrostatic pressure, or fluid shear stress. Individual cells are now recognized as being mechanically sophisticated, integrating mechanosensory stimuli to alter physiological, biochemical, and genetic processes, and having the ability to dynamically alter their mechanical properties. In fact, the mechanical properties of the cell are integral to the transduction of mechanical stress as cells sense and respond to their physical environment. The link between mechanical properties of the cell, mechanical stress acting on the cell, and the resulting biochemical and molecular responses is important for cell functioning and also implicated in cellular pathologies.

In this study, the relationship between cell biomechanics and physiological sensitivity was investigated in dinoflagellates, alveolate protists whose bioluminescence serves as a cellular reporter of one of the fastest-known mechanosensitive systems, with only a 15 to 20 ms delay between stimulus and response (1–3). The mechanotransduction mechanism and the link between cell morphology and mechanosensitivity are poorly characterized. Mechanical stress is hypothesized to activate GTP-binding proteins (4) by increasing the fluidity of the plasma membrane (5) as in mammalian endothelial cells sensing blood flow (6–8), a process that appears involve membrane thinning rather than changes in membrane curvature (9). Pharmacological studies suggest that the bioluminescence signaling pathway involves the activation of voltage-sensitive and stretch-sensitive integral membrane proteins (9–11), an increase in cytoplasmic [Ca^{2+}] by release from intracellular stores (11), and depolarization of the vacuole membrane to generate a propagating action potential (3,12). The vacuolar membrane action potential is hypothesized to open voltage-gated proton channels (13) to acidify the scintillons, vesicles that contain the substrate luciferin and catalyst luciferase involved in the luminescent chemistry (14–17). The decreased pH in the scintillons activates the luciferase, whose activity is pH dependent, and in some dinoflagellate species dissociates luciferin from its binding protein (14,18,19). Overall, dinoflagellate bioluminescence is an extremely rapid, noninvasive tool for evaluating the sensitivity and mechanisms of response of individual cells.

In nature, the bioluminescence of dinoflagellates, the most common sources of bioluminescence in coastal regions (20,21), functions as a predator defense strategy. Bioluminescent flashes have a flash bulb effect to disrupt predator feeding (22–26) and also act as a burglar alarm to attract secondary visual predators that prey on the initial grazers (27–31). In this context bioluminescence appears to be stimulated by direct predator contact rather than flows associated with a predator feeding current (32,33).

Dinoflagellate bioluminescence is also stimulated by flows with high levels of shear stress, including the

Submitted September 11, 2014, and accepted for publication February 2, 2015.

*Correspondence: tessonben@gmail.com or mlatz@ucsd.edu

Benoit Tesson's present address is INRA, UMR1319 Micalis, F-78352 Jouy-en-Josas, France.

Editor: Klaus Hahn.

0006-3495/15/03/1341/11 $2.00

http://dx.doi.org/10.1016/j.bpj.2015.02.009

boundary layers of swimming animals (34,35), ship wakes (36), and breaking waves (35,37). Based on studies using fully characterized flow fields with quantified levels of flow stress, the bioluminescence response starts in flows with fluid shear stresses of 0.02 to 0.3 N m^{-2}, depending on the dinoflagellate species (32,38,39). Dinoflagellate bioluminescence is sensitive to the rate of change of flow stress, suggesting a slow inactivation process that results in decreased levels of light emission with lower rates of increase in flow stress (33).

Laboratory approaches using fully characterized flow fields are amenable to populations of cells but do not allow the study of individual cells or the precise characterization of the local mechanical stress triggering flash responses. Additionally, flow approaches are suitable to studying flow-stimulated bioluminescence but are not necessarily relevant to mechanical stimulation because of predator contact. A sophisticated approach to investigate the effect of mechanical forces on individual cells is atomic force microscopy (AFM), a high-resolution tool for imaging surfaces at the nanoscale. A probe mounted on a cantilever feels a surface over which it is scanned. Forces between the tip and sample cause deflection of the cantilever that is detected by a laser on a photodetector. Thus AFM can image a surface with nanometer resolution. In addition, AFM can also be used to apply known forces and has become the tool of choice for probing and manipulating a wide variety of cells and macromolecules (40). Although there are many methods available for applying a mechanical stimulus to individual cells, the advantages of AFM are that it can apply local forces with high spatial resolution using relevant testing conditions for live cells, in this case while immersed in seawater. The resulting force-distance curve is used to calculate deformation and elastic modulus of the sample, making AFM one of the most effective tools for measuring the mechanical properties of cells (41).

The objective of this study is to develop AFM as a tool to investigate the relationship between stimulation parameters and physiological sensitivity of individual dinoflagellates, whose in vivo bioluminescence has been used as a reporter of mechanical stress in oceanic and engineering applications (36,42–44). Local stimulation using a colloidal probe was applied to single cells of the dinoflagellate *Pyrocystis lunula* attached to a solid surface. This species was selected for testing because it exists in cultures primarily in a nonmotile cyst stage (45,46), unlike most dinoflagellates, which exist in a flagellated swimming stage, and this particular strain was negatively buoyant, facilitating its attachment to a surface for testing. Results indicate that the velocity of the applied mechanical stress and its magnitude are important in determining cell stimulation. By measuring the mechanical properties of the cells, we were able to correlate the characteristic of the mechanical stimulation triggering a response with the viscoelastic properties of the cells. To our knowledge, this study establishes AFM as a tool to study mechanosensitivity in luminescent dinoflagellates at fast timescales, providing a new perspective for the understanding of this phenomenon and the mechanotransduction process in general.

MATERIALS AND METHODS

Test organism and culture conditions

Cultures of *Pyrocystis lunula* Schütt (47) were grown in half-strength Guillard's f/2 medium minus silicate in an environmental chamber maintained at 20°C with a 12:12 h light:dark cycle. Only cultures in midexponential growth phase (i.e., 2 weeks after inoculation) were used for testing. The bioluminescence of *P. lunula* and that of most dinoflagellates is under circadian regulation, with light emission only during the dark phase of the photoperiod (48,49). Cells were prepared for testing toward the end of the light phase, when the bioluminescence system is inactive. Cells were adhered to polystyrene petri dishes (Thermo Fisher Scientific, Waltham, MA) by adding 0.1 ml drops of culture that remained undisturbed in the light for 1 h. Dishes were then rinsed with aged Scripps Pier filtered seawater (FSW) and refilled with 6 ml of FSW. Dishes were placed in the AFM room at the beginning of the dark phase where they remained undisturbed until testing.

Cell imaging

Bioluminescence was imaged by a Cascade:512B digital low-light camera system (Photometrics, Tucson, AZ) attached to the side port of the Zeiss AXIO Observer.A1 inverted microscope (Carl Zeiss Microscopy, Thornwood, NY). A Fura2 filter cube with 540 nm long-wavelength cutoff attenuated the AFM red laser illumination from reaching the camera and interfering with observing the bioluminescence, which for *P. lunula* has a maximum emission at 472 to 475 nm (50,51).

Camera operation was controlled through Metamorph v6.3 software (Molecular Devices, Sunnyvale, CA), which was also used for image analysis. Camera settings were 10 MHz digitizer, maximum gain, intensifier setting of 3000, and 20 ms frame duration, with a 256 × 256 pixel field of view. Typically 200 frames were obtained for a single indentation and retraction of the cantilever probe. Cells were imaged with a Plan NEOFLUAR 40x/0.75 n.a. (Carl Zeiss Microscopy) objective.

Cell size was determined from a white light image of each cell obtained with the AFM probe out of view, and calculated based on scale calibration using a stage micrometer. Cell length and width were based on maximum values, whereas projected surface area was obtained after outlining the cell periphery.

Cell measurements and bioluminescence stimulation using AFM

A Bioscope catalyst Atomic Force Microscope (Bruker, Billerica, MA) was coupled with the inverted microscope for imaging and force spectroscopy. The surface of the dinoflagellate cell was imaged in Scanasyst mode using a Bruker SNL-A cantilever (2 nm tip diameter). For the force spectroscopy experiments, various types of probes with different spring constants and modifications (e.g., sharp tip, tipless, beads of various diameters) were tested. The best results were obtained using a colloidal probe, consisting of a silicon cantilever with a spring constant of 45 N m^{-1} attached to a 10.3 μm diameter glass bead (AppNano model ACTLGG, Applied NanoStructures, Mountain View, CA). The cantilever spring constant was determined using the dimensional method and the diameter of the glass beads measured by mean ± SE. The deflection sensitivity of the cantilever was calibrated in liquid on a sapphire surface. The cantilever was positioned so that it contacted the cell in the area above the nucleus (Fig. 1); this region provided a flat surface allowing proper contact between the cell and the AFM probe. Contacting the cell in other areas resulted in cell movement

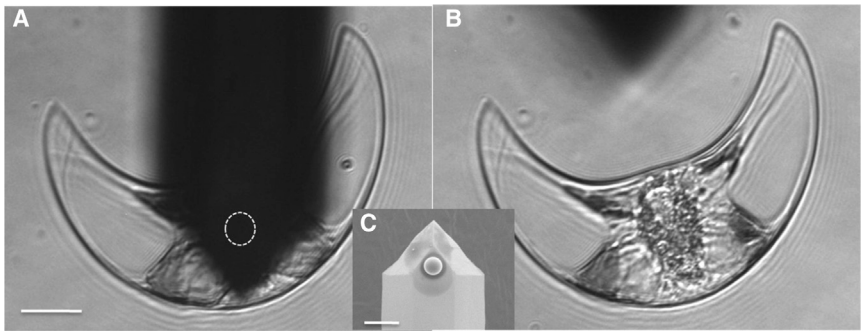

FIGURE 1 Images of a living *Pyrocystis lunula* cell. (*A*) Cantilever probe with approximate position of attached glass sphere (*circle*) positioned over the cell. (*B*) Same cell without the cantilever. (*C*) Scanning electron micrograph of the cantilever with attached 10 μm diameter glass sphere. Scale bar for all panels is 20 μm.

causing inadvertent stimulation. The contact area was determined using the formula to calculate the surface area of a spherical cap: $2\pi \times r \times h$ where r is the radius of the probe and h the depth of indentation. Cell deformation was determined from the force curve.

The objective of force experiments was to study mechanosensitivity based on the magnitude of the applied force and the rate at which the force was applied, using bioluminescence as the reporter of cell physiological response. Three types of force experiments were performed. Each experiment was performed using the same conditions and identical probe. The ramp size (z motion of the cantilever) was set at 10 μm and the maximum applied force of 14.5 μN and velocity of 390 μm s^{-1} (equivalent to a ramp rate of 19.5 Hz) were determined according to the system and cantilever characteristics.

For the first experiment, the stimulation velocity was kept constant at 390 μm s^{-1} while a series of single indentations with increasing force from 1.6 to 14.5 μN was applied until bioluminescence was stimulated. Then a subsequent stimulus at the maximum velocity (390 μm s^{-1}) and force (14.5 μN) was applied to the same cell to elicit a second flash response.

For the second experiment the force was maintained at the maximum of 14.5 μN while a series of single indentations with increasing velocity from 20 to 390 μm s^{-1} was applied until bioluminescence was triggered. Then a subsequent stimulus was applied at the maximum force and velocity to elicit a second flash response.

The third experiment evaluated the effect of repeated stimulation on the same cell. A series of repetitive indentations over a period of 20 s was performed at the maximum force of 14.5 μN with a 1 s delay between each stimulus; one group of cells was stimulated at a velocity of 20 μm s^{-1} while a second group was stimulated at 390 μm s^{-1}. For the series at a ramp rate of 20 μm s^{-1}, a final single stimulus was applied at a velocity of 390 μm s^{-1} to verify responsiveness of the cell.

Each flash was analyzed for intensity and kinetic parameters. Maximum flash intensity was obtained from the frame with the highest intensity by taking the average value of all pixels involved in the light emission. Response kinetics were calculated from analysis of the video record, with each frame representing 20 ms duration. Rise time was based on the number of frames from the initiation of the response to maximum intensity. Dinoflagellate flashes undergo an exponential decay in light intensity (12,52,53). Decay time was based on the period from maximum intensity to 90% of maximum. Decay rate was calculated as the inverse of the 90% decay time.

Unless otherwise stated, values represent arithmetic means with standard deviation. Simple comparisons were made using Student's *t*-test, whereas correlations were based on simple least-squares linear regressions using JMP v.11 (SAS Institute, Cary, NC). Statistical significance was based on $\alpha = 0.05$.

Cell mechanical properties

To determine the elasticity of cells in the same conditions, at the end of each series of bioluminescence measurements a force curve was obtained with a maximum force of 6.4 μN and velocity of 20 μm s^{-1}. The Hertz model for spherical indenter was used to fit the curves and determine the elastic modulus. The Poisson ratio was fixed at 0.5. Nanoscope analysis software v.1.4 was used to fit the force deformation curves.

Additionally, we investigated the effect of stimulation velocity on the mechanical properties of the cells and determined their viscoelastic properties by performing stress relaxation tests. These measurements were performed on the same six cells. For each cell, two single force curves were obtained with a force of 14.5 μN and velocities of 20 and 390 μm s^{-1}. One single force curve was obtained at 6.4 μN and 20 μm s^{-1} to determine Young's modulus. Finally, a stress relaxation test was realized. The indenter was brought in contact with the cell at a velocity of 20 μm s^{-1} until a maximum force of 14.5 μN was obtained. Constant deformation was maintained for 10 s while the force applied was recorded.

Based on the stress relaxation curves, elastic modulus, E, was calculated from force values using the Hertz theory for a spherical indenter. Then the stress relaxation curves were fitted using least squares to a nonlinear regression with LAB Fit V.7.2.48 software (Universidade Federal de Campina Grande, Paraiba, Brazil), using a viscoelastic model that consists of a parallel arrangement of two Maxwell elements and a spring as follows:

$$E(t) = E_0 + E_1 \exp(-t/\tau_1) + E_2 \exp(-t/\tau_2). \quad (1)$$

This model allowed us to obtain the viscoelastic parameters of cells including the relaxation time τ_1 and τ_2, the elastic moduli E_0, E_1, and E_2, and the parameters of viscosity μ_1 and μ_2, as follows:

$$\mu = E * \tau. \quad (2)$$

RESULTS

Cell wall structure

The surface layer of *P. lunula* was quite homogeneous, displaying a grid pattern formed by the cellulose network present underneath the surface layer (Fig. 2 *A*). Imaging at high resolution revealed domes and ridges with an average height of 5.4 nm, width of 100 to 150 nm, and Roughness root mean square (Rrms) of 1.59 nm (Fig. 2, *A* inset and *B*). Occasionally we observed attached needle-like structures ~1.8 μm in length that could be discharged trichocysts (Fig. 2 *C*), rod-shaped structures that are a common type of extrusome in dinoflagellates (54,55) including *P. lunula* (56).

Stimulation of bioluminescence

Overall, bioluminescence was triggered in 76% of tested cells (N = 42) for single indentations with a maximum force

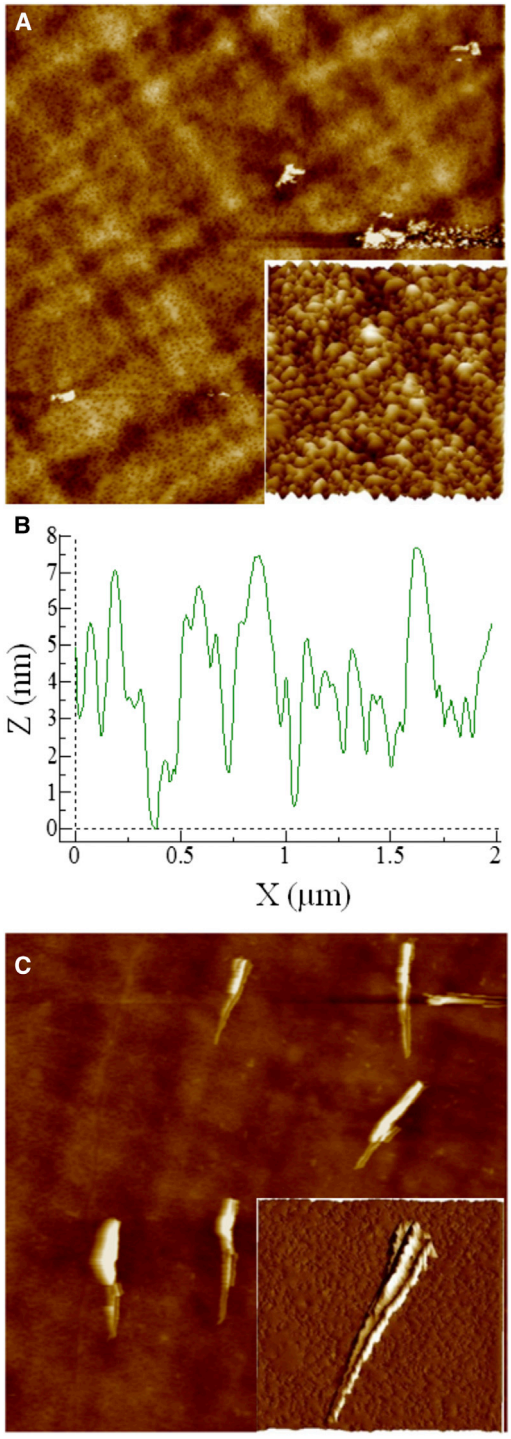

FIGURE 2 Structure of the living *Pyrocystis lunula* cell surface as imaged by atomic force microscopy. (*A*) Low-resolution image showing a grid pattern. Scan size is 10 μm. Inset: high-resolution image of the cell surface. Scan size is 2 μm. (*B*) Height (Z) profile of the cell surface from (*A*) inset. (*C*) Low-resolution image of elongated structures, which may be extruded trichocysts, occasionally imaged on the cell surface of *Pyrocystis lunula* by atomic force microscopy. Scan size is 9.4 μm. Inset: high-resolution image of a trichocyst. Scan size is 2 μm. To see this figure in color, go online.

of 14.5 μN and velocity of 390 μm s^{-1} (Movie S1 in the Supporting Material). Light emission always originated from a circular region in the vicinity of the nucleus.

Experiment 1: sensitivity based on stimulus force

For this experiment, cells were indented at the maximum velocity of 390 μm s^{-1} allowed by the system, with an initial applied force of 1.6 μN that was increased in increments with each indentation until a flash was observed. For all cells tested, the flash response occurred at a force threshold of 7.2 $\pm$ 3.4 μN, corresponding to a cell deformation of 2.1 $\pm$ 0.65 μm and a contact area of 68 μm^2 or 1.4% of the cell surface; the time to reach maximum deformation once the cell surface was contacted was 6.1 $\pm$ 1.8 ms (Fig. 3 *A*; Table S1). The maximum intensity of the response did not vary with the magnitude of the applied force ($P = 0.79$) indicating that the flash was an all-or-nothing response.

Experiment 2: sensitivity based on stimulus velocity

To determine the effect of stimulus velocity on cell stimulation, cells were indented at a constant maximum force of 14.5 μN, with an initial velocity of 20 μm s^{-1} that was increased in increments with each indentation until a flash was observed. For all cells tested, the flash response occurred at a threshold velocity of 118 $\pm$ 78 μm s^{-1}, corresponding to a cell deformation of 3.1 $\pm$ 0.3 μm and contact area of 100.5 $\pm$ 8.5 μm^2; the time for the probe to travel from the surface of the cell to the maximum deformation was 47.1 ms (Fig. 3 *B*; Table S2). The maximum intensity of the response did not vary with ramp rate ($P = 0.16$) indicating that the flash was an all-or-nothing response.

The parameters of the cell flash response were similar for the two experiments ($P > 0.05$). The flash response was always present in the subsequent video frame after probe contact, representing a delay between stimulation and response of 20 ms or less, consistent with previous findings using different stimulation strategies (1,3,57). There was a significant difference between experiments in rise time, the time to maximum flash intensity ($t_{20} = 2.4$, $P < 0.03$), which was 44.0 $\pm$ 2.9 ms for experiment 1 and 53.3 $\pm$ 2.7 ms for experiment 2. However, considering that the time resolution of these measurements was 20 ms, and all response rise times were either 40 or 60 ms, no functional importance is placed on the difference. Pooling the results for the two experiments, rise time was 49.1 $\pm$ 10.2 ms ($N = 22$) and 90% decay time was 379 $\pm$ 52.2 ms, equivalent to a decay rate of 2.7 $\pm$ 0.3 s^{-1}.

There was no significant correlation of response kinetics (i.e., rise time, decay rate, and 90% decay time) with cell area ($P > 0.6$). Maximum response intensity increased with cell area in a log-log relationship ($R^2 = 0.251$, $F_{1,20} = 6.71$, $P = 0.02$) as expected, because larger cells have a greater bioluminescence capacity (52,58–60). Elastic modulus (y) increased with cell area (x) as $y = 0.135 + 8.8 \times 10^{-5} * x$ ($R^2 = 0.203$, $F_{1,20} = 5.08$, $P = 0.04$).

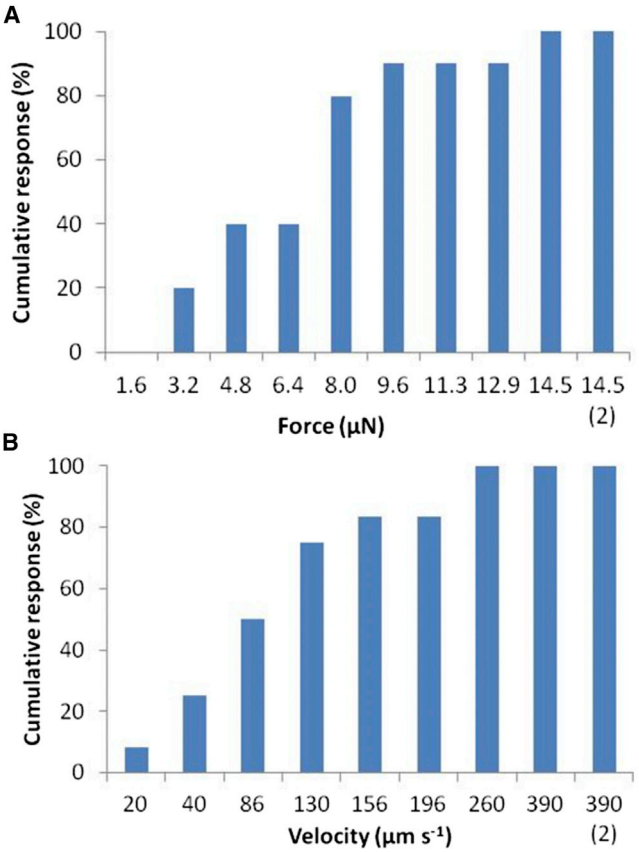

FIGURE 3 Cumulative percentage of *Pyrocystis lunula* cells responding at (*A*) constant stimulation velocity of 390 μm s^{-1} and various forces, and (*B*) constant force of 14.5 μN and various velocities. For each experiment, the second stimulus at maximum force and velocity "(2)" always elicited a response. To see this figure in color, go online.

Experiment 3: repeated stimulation

To investigate the effect of multiple stimulation on cell response and to confirm the effect of stimulation velocity, we performed an experiment where cells were indented at least seven times at the maximum force of 14.5 μN and a velocity of 20 or 390 μm s^{-1} (Fig. 4 and Table S3). For a velocity of 20 μm s^{-1}, no cells were stimulated (N = 6), although all but one cell was stimulated by a subsequent indentation at a velocity of 390 μm s^{-1}, verifying that the cells were excitable. When the same experiment was performed for a velocity of 390 μm s^{-1} using different cells, five out of seven cells were stimulated, with all responding cells producing a flash for the first stimulus. The number of flashes per cell was highly variable, ranging from one to six flashes. This experiment confirmed the importance of stimulus velocity for cell stimulation, because cells did not respond at the low velocity even though the force was maximal.

Pyrocystis spp. exhibits a first flash phenomenon, where the first flash that is elicited has a higher intensity and longer duration than subsequent flashes (52). This pattern was observed in our study (Fig. 4 *D*), where the first flash was more than six times brighter with about a three times greater duration than subsequent flashes.

Mechanical properties

For an applied force of 6.4 μN and velocity of 20 μm s^{-1}, Young's modulus for the region above the nucleus was 0.56 $\pm$ 0.14 MPa (N = 28 cells) (Fig. 5 *A*).

To better understand the effect of probe velocity on cell stimulation, we performed force deformation curves at a force of 14.5 μN for velocities of 20 and 390 μm s^{-1} (Fig. 5 *B*). Deformation for a velocity of 20 μm s^{-1} was 3.5 $\pm$ 0.46 μm (N = 6 cells) whereas that for a velocity of 390 μm s^{-1} was 3.13 $\pm$ 0.37 μm (Table S4). The 0.37 $\pm$ 0.11 μm difference was statistically significant (paired *t*-test, $t_8 = 12.3$, $p < 0.0001$). We attributed this difference to the relaxation of the cell at the lower stimulation velocity.

To directly measure cell relaxation, the same cells were subjected to stress relaxation tests to determine the viscoelastic properties of the cells and the relaxation times (Fig. 5 *C*). The force required to maintain a constant deformation was measured for 10 s. The indentation moduli were calculated using the Hertz theory for spherical indenter. Initially the elastic moduli exhibited a rapid decrease, followed by a slow decrease to finally stabilize at around 9 s. A viscoelastic model consisted of two sets of dashpot and a spring, representing slow and rapid relaxation, respectively, as well as a single spring to describe the elasticity at equilibrium was used to fit the data (Fig. 5, *C* and *D*). The correlation coefficient for the fit ranged from 0.999 to 0.988. Based on model calculations, the relaxation times were 0.132 $\pm$ 0.046 s and 3.09 $\pm$ 0.73 s, the moduli at equilibrium was 0.318 $\pm$ 0.124 MPa, and the instantaneous modulus E_1 was 0.097 $\pm$ 0.039 MPa and modulus E_2 was 0.026 $\pm$ 0.011 MPa. The viscosity parameters were calculated as $\mu_1 = 14.2 \pm 9.9$ KPa s and $\mu_2 = 83 \pm 42.1$ KPa s (Table S4).

DISCUSSION

Dinoflagellate bioluminescence as a cellular reporter of mechanical stress

Mechanical forces affect cellular biochemistry, physiology, and gene expression (61–65). Single-cell model systems, which are useful for deciphering the mechanisms involved in mechanosensitivity, present a challenge for monitoring the effector response. Typically mechanosensitivity is measured by monitoring activity within the signaling pathway, such as using fluorescent dyes for measuring membrane viscosity, cytoplasmic $[Ca^{2+}]$, or pH; performing electrical recordings of membrane voltage; or monitoring fluorescent fusion reporter proteins (66–68). Dinoflagellate bioluminescence is a powerful whole-cell reporter of mechanical stress because light production represents the final step of a rapid, intrinsic mechanosensing pathway. Bioluminescence represents the effector response of the cell, not an intermediate

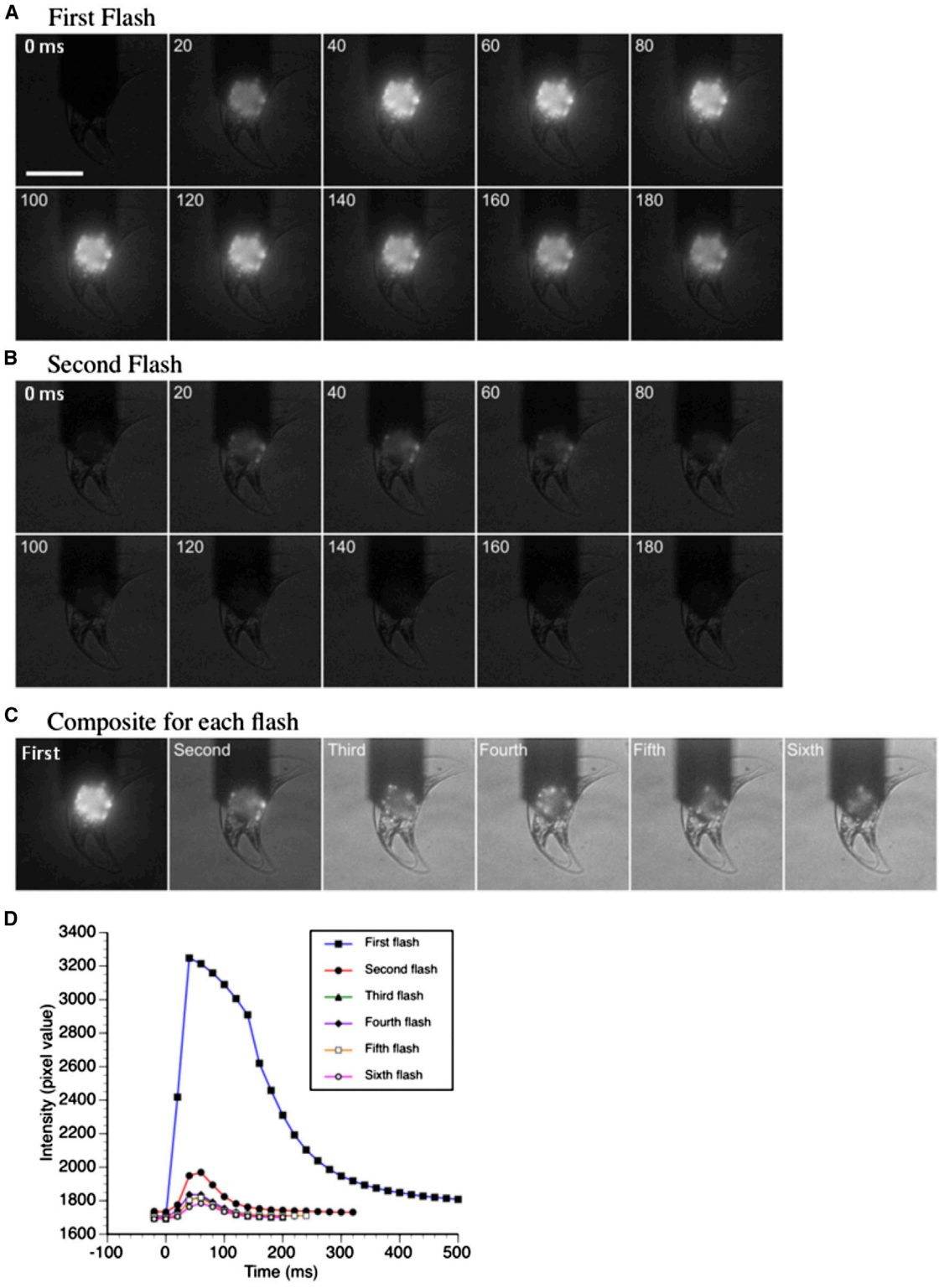

FIGURE 4 Sequence of bioluminescence produced by a *Pyrocystis lunula* cell stimulated by the atomic force microscope probe. (*A*) The probe contacts the cell at time 0 with a force of 14.5 μN and velocity of 390 μm s^{-1}. A flash is visible in the next frame at time 20 ms, reaches maximum intensity at time 40 ms, and then undergoes slow decay. For this cell, the flash intensity decayed to 90% of maximum in 220 ms. (*B*) The second flash produced by the identical cell exhibited a lower intensity and shorter duration. Both (*A*) and (*B*) have the identical intensity scaling. (*C*) Composite of the six flashes produced by the identical cell based on the maximum intensity of emission. The images are autoscaled so that the background appears brighter when the bioluminescence is dimmer. Scale bar for all panels is 50 μm. (*D*) Time course of each of the flashes, based on average pixel intensity for the region of bioluminescence. To see this figure in color, go online.

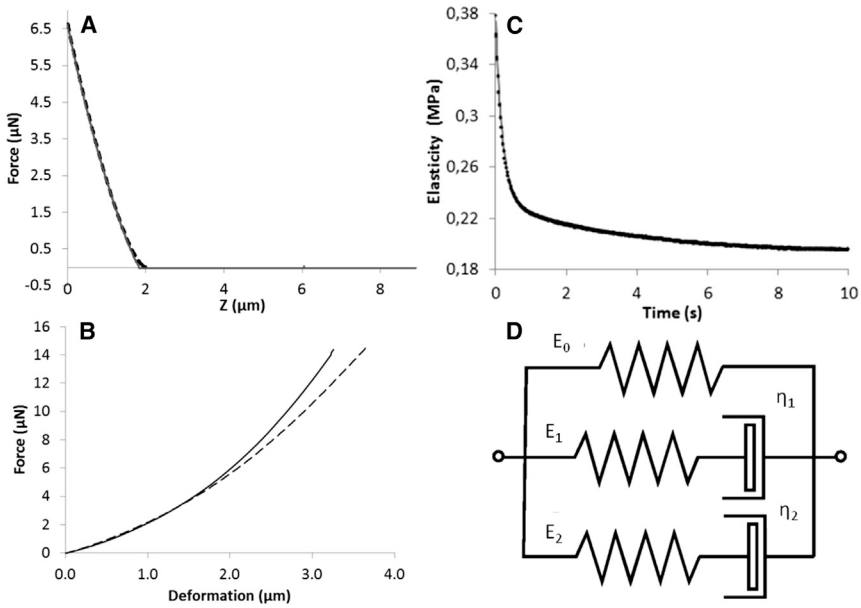

FIGURE 5 Viscoelastic properties of *Pyrocystis lunula* cells. (*A*) Force curve (*solid line*) fitted with the Hertz model (*dashed line*) used to calculate Young's modulus. (*B*) Force deformation curves from a single cell measured for velocities of 20 (*dashed line*) and 390 μm s^{-1} (*solid line*). (*C*) Stress relaxation curve (*dots*) of a living cell fitted using the model described in *D* (*solid line*). (*D*) Viscoelastic model consisting of two sets of dashpot and a spring and a single spring arranged in parallel.

step such as a change in membrane fluorescence or voltage, or an increase in cytoplasmic [Ca^{2+}]. The light emission, which consists of one or more flashes with a duration of ~500 ms and emission of 5×10^8 photons for *P. lunula* (M.I. Latz, unpublished data), is clearly imaged or measured from individual cells. The most thorough characterization of the mechanosensitivity of dinoflagellate bioluminescence has used fully characterized flow conditions to determine thresholds of stimulation and examine the scaling of bioluminescence intensity with the magnitude of fluid shear stress (32,33,38,39). However, this approach using populations of cells provides limited insight into the responses of individual cells (69), and it is unclear how bulk fluid forces are related to local forces and cell deformation. The major contribution of this study is to use AFM to apply known forces to marine cells in which naturally occurring bioluminescence is used as a reporter of mechanosensitivity. Therefore, mechanosensitivity can be quantified in the context of the mechanical property of the cells, also measured by AFM. This approach provides the capability for experimental investigation of dinoflagellates, possessing one of the fastest-known mechanosensitive signaling pathways, operating on timescales of 10 to 20 ms (3,12,57). As dinoflagellates are simple Eukaryotes, it is interesting to consider elements of their signaling pathway that have been conserved in higher organisms. To our knowledge, this work establishes a framework for future pharmacological investigations and the development of dinoflagellates as a new model for the study of mechanotransduction mechanisms.

Cell mechanical properties

Cell stiffness of *Pyrocystis lunula*, as measured with the AFM spherical probe, yielded a Young's modulus of 0.56 MPa. This value is much higher than 0.5 to 200 kPa for cultured animal cells (70–72) but is consistent with that of cells possessing a cell wall such as yeast and plants (73,74). For example, the stiffness of wild-type yeast is 0.6 MPa, whereas the organic part of the diatom cell wall varies from 0.1 to 0.5 MPa (74–76). In *Arabidopsis*, Young's modulus of the cell wall varies from 1.5 to 5 MPa using a pyramidal indenter and from 0.1 to 0.7 MPa with a spherical probe (77,78).

Cells of *Pyrocystis lunula* exist mainly in a cyst form and have an outer cell wall ~400 nm thick, with a thin outer layer composed of dinosporin, a highly resistant carbohydrate based polymer, and a thick inner layer of crossed parallel cellulose fibrils (79,80), which appeared as a grid pattern in this study, the first time, to our knowledge, that these layers have been imaged in their native state. Proximal to the cell wall lies the protoplast, which contains actin filaments and microtubules used to support and transport organelles (81–83). The contribution of the various components of the cytoskeleton to cell stiffness remains to be determined.

Mechanosensing mechanism: linking cell mechanics to mechanosensitivity

In this study we found that the rate of stimulation plays a critical role in cell response. Most of the cells were stimulated at maximum force by high but not low stimulation velocity. The rate-dependent response may be attributable to the viscoelastic properties of the cells. Deformation was 370 nm greater at the low stimulation velocity of 20 μm s^{-1} compared with the high velocity of 390 μm s^{-1}, representing ~10% of the total deformation and indicating that cell relaxation occurred. The low stimulation velocity

resulted in a longer contact time of 171 ms compared with a contact time of only 6 ms at the high stimulation velocity. A viscoelastic model of the cell that consisted of two Maxwell elements and a spring arranged in parallel was used to fit the stress relaxation curves, with fast (132 ms) and slow (3.1 s) components of relaxation. According to a rate dependent response, at low stimulation rates stress relaxation would result in energy dissipation whereas at high stimulation rates, the stress accumulates.

Mechanotransduction in dinoflagellates is not well understood. Pharmacological treatments provide evidence for the role of GTP-binding proteins (4) and stretch-activated ion channels (9), both most likely localized in the plasma membrane. For our viscoelastic model, which explains velocity dependent mechanosensor activation based on modeling the cell membrane as a dashpot, high stimulation velocity would result in membrane tension increase leading to a conformational change of mechanosensors localized in the membrane that trigger bioluminescence response (Fig. 6). Our results and this model are consistent with the role of a membrane-localized mechanosensor. The flash was not graded in amplitude or kinetics but was an all-or-nothing cellular response, consistent with previous studies using unquantified levels of mechanical stimulation (52,53). There was minimal effect of stimulus parameters on flash response characteristics. This all-or-none feature enhances the value of dinoflagellate bioluminescence as a cellular reporter of mechanical stress.

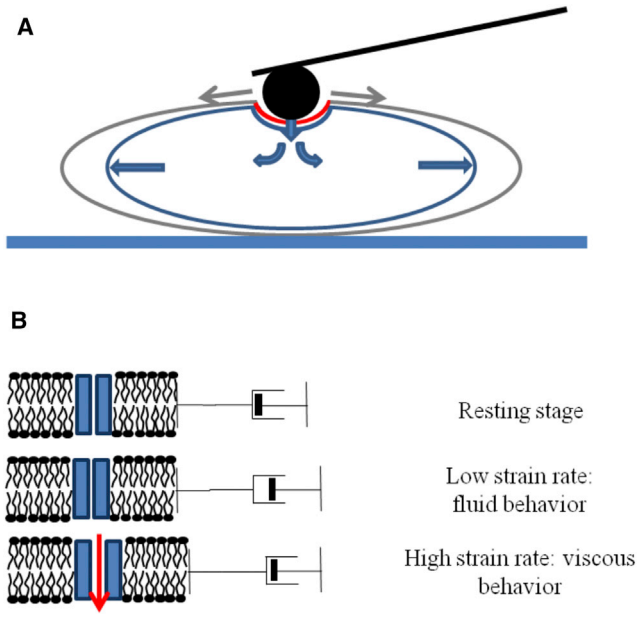

FIGURE 6 Effect of compressive force applied by atomic force microscopy. (*A*) Schematic representation of cell deformation by a colloidal probe showing relaxation mechanism. Gray arrows represent relaxation of the cell wall (*gray*) and blue arrows represent relaxation of the protoplast (*blue*). (*B*) Hypothetical model for strain rate dependent conformational change of mechanosensor. To see this figure in color, go online.

Other velocity dependent responses have been observed in osteoblast cells, using calcium release as a reporter for cell response (84), and in myoblast cells, where mechanosensory elements with distinct biomechanical properties allow cells to differentiate mechanical stimuli with distinct properties (85). In the myoblast study one mechanosensor activation required high strain whereas the other one required high stimulation rate for conformational change.

The dinoflagellate bioluminescence system is characterized by its fast response time. In this study, the maximum flash response occurred in 40 to 60 ms. The 20 ms time resolution of image acquisition was too coarse to measure the delay from mechanical stimulus to the beginning of the flash response, but previous studies have measured response delays of 15 to 22 ms (3,57,86), with minimum delays of 8 to 12 ms for several strains of *Lingulodinium polyedrum* (57).

Comparing flow-induced and compressive mechanosensitivity

In the ocean environment, dinoflagellate bioluminescence is stimulated by mechanical stress in the form of direct predator contact or fluid shear stress (32,39,87). The flow-stimulated bioluminescence of *P. lunula* has not been quantified. However, *P. fusiformis*, which has a similar cell wall morphology, has been studied in fully developed laminar simple Couette and pipe flows, where it has a response threshold in flows with a shear stress of 0.06 to 0.09 N m^{-2} (32,38). Assuming a cell surface area for a 1 mm long *P. fusiformis* cell of 1.1×10^5 μm^2, then the fluid force acting across the entire cell surface is 6.6×10^{-2} μN. Another flow approach used a microfluidic device to immobilize cells at a barrier, where they experienced hydrodynamic drag (57). The lowest flow velocity tested, which stimulated 50% of cells of the dinoflagellate *Lingulodinium polyedrum*, applied an estimated tensile force of 4.0×10^{-2} μN, equivalent to a stress of 10.4 N m^{-2} for a cell surface area of 3850 μm^2. These response thresholds are based on calculated flow properties for fully developed flow rather than forces acting on the cell, which are unknown. For AFM stimulation, a threshold force of 7.2 μN with a contact area of 68 μm^2 corresponded to a local stress of 1.1×10^5 N m^{-2}. It is difficult to compare the effect of fluid shear and compressive stress because the flow stimulation approach does not provide any information about cell deformation and it assumes that the entire cell surface area experiences a similar level of shear stress.

Cell response because of flow stimulation may represent mechanosensitivity integrated over the entire cell surface, rather than local stimulation in the case of AFM. The cell response may require the activation of a minimum number of mechanosensors; perhaps increasing the region of stimulation would lead to a decrease in the threshold level of mechanical stress. Mammalian endothelial cells, which experience shear stress present in blood flow, respond to a

similar range of fluid shear stress (32,39,65,88,89) as do dinoflagellates, despite lacking the cell wall present in dinoflagellates and having a cell stiffness of 1-10 kPa (70,71), approximately two orders of magnitude less than in dinoflagellates. Flow forces act directly on the membrane by increasing its fluidity (5,6) and possibly activate integral membrane proteins, whereas compression first contacts the cell wall; these different mechanisms of activation may explain the higher threshold for contact stimulation. Until more is known about how mechanical stress is sensed by the cell, it is difficult to compare different modes of stimulation. However, comparisons so far indicate that the cell stimulation requires greater compressive forces than fluid shear forces calculated from flow properties.

CONCLUSION

To our knowledge, this is the first study to apply AFM for studying the link between mechanosensitivity and mechanical properties of marine cells. We developed a new method that allows us to study mechanosensitivity in organisms possessing an extremely rapid mechanosensing system, in which in vivo light emission serves as a whole-cell reporter of cell response. We described the conditions of stimulation required to trigger a response and showed that both the level of stress and speed of stimulation are critical factors. This initial study paves the way for future pharmacological investigations that will help decipher the biochemical steps involved in cell signaling. The velocity dependent response observed has physiological and ecological significance. Indeed, it allows us to build a model that takes into account the effect of mechanical properties of the cell on mechanosensing. Additionally, in an environmental context, the velocity dependence of stimulation modulates the sensitivity of cells to mechanical stress and limits unnecessary cell response. Cell stimulation by compressive forces is relevant to the ecological role of dinoflagellate bioluminescence as a predator defense strategy, where the primary stimulus is attributable to mechanical stress from predator contact, as shear stress levels when the cell is entrained in a predator feeding current are too low to be stimulatory (32,33). Thus this study using mechanical stress generated through direct contact of the cell with the AFM cantilever is relevant to how the cell encounters mechanical stimuli imparted by the predator.

SUPPORTING MATERIAL

Four tables and one movie are available at http://www.biophysj.org/biophysj/supplemental/S0006-3495(15)00169-1.

ACKNOWLEDGMENTS

We thank M. Hildebrand for the opportunity to carry out this study, J. Shaw of Bruker Corp. for technical assistance with operation of the atomic force microscope, J. Baxter for technical assistance with organism handling, and J. Rohr for helpful comments on the manuscript.

This work was supported by the U.S. Air Force Office of Scientific Research MURI grant FA9550-10-1-0555 (B.T.), the National Science Foundation grant 1205930 (M.I.L.), and UC San Diego Academic Senate research funds (M.I.L.).

REFERENCES

1. Eckert, R. 1965. Bioelectric control of bioluminescence in the dinoflagellate *Noctiluca*. II. Asynchronous flash initiation by a propagated triggering potential. *Science.* 147:1142–1145.
2. Latz, M. I., M. Bovard, …, A. Groisman. 2008. Bioluminescent response of individual dinoflagellate cells to hydrodynamic stress measured with millisecond resolution in a microfluidic device. *J. Exp. Biol.* 211:2865–2875.
3. Widder, E. A., and J. F. Case. 1981. Bioluminescence excitation in a dinoflagellate. *In* Bioluminescence Current Perspectives. K. H. Nealson, editor. Burgess, Minneapolis, MN, pp. 125–132.
4. Chen, A. K., M. I. Latz, …, J. A. Frangos. 2007. Evidence for the role of G-proteins in flow stimulation of dinoflagellate bioluminescence. *Am. J. Physiol. Regul. Integr. Comp. Physiol.* 292:R2020–R2027.
5. Mallipattu, S. K., M. A. Haidekker, …, J. A. Frangos. 2002. Evidence for shear-induced increase in membrane fluidity in the dinoflagellate *Lingulodinium polyedrum*. *J. Comp. Physiol. A Neuroethol. Sens. Neural Behav. Physiol.* 188:409–416.
6. Haidekker, M. A., N. L'Heureux, and J. A. Frangos. 2000. Fluid shear stress increases membrane fluidity in endothelial cells: a study with DCVJ fluorescence. *Am. J. Physiol. Heart Circ. Physiol.* 278:H1401–H1406.
7. Gudi, S., J. P. Nolan, and J. A. Frangos. 1998. Modulation of GTPase activity of G proteins by fluid shear stress and phospholipid composition. *Proc. Natl. Acad. Sci. USA.* 95:2515–2519.
8. Chachisvilis, M., Y.-L. Zhang, and J. A. Frangos. 2006. G protein-coupled receptors sense fluid shear stress in endothelial cells. *Proc. Natl. Acad. Sci. USA.* 103:15463–15468.
9. Jin, K., J. C. Klima, …, M. I. Latz. 2013. Pharmacological investigation of the bioluminescence signaling pathway of the dinoflagellate *Lingulodinium polyedrum*: evidence for the role of stretch-activated ion channels. *J. Phycol.* 49:733–745.
10. von Dassow, P. 2003. Regulation of bioluminescence in the dinoflagellate *Lingulodinium polyedrum*. PhD thesis. University of California San Diego.
11. von Dassow, P., and M. I. Latz. 2002. The role of $Ca^{(2+)}$ in stimulated bioluminescence of the dinoflagellate *Lingulodinium polyedrum*. *J. Exp. Biol.* 205:2971–2986.
12. Eckert, R. 1965. Bioelectric control of bioluminescence in the dinoflagellate *Noctiluca*. I. Specific nature of triggering events. *Science.* 147:1140–1142.
13. Smith, S. M. E., D. Morgan, …, T. E. Decoursey. 2011. Voltage-gated proton channel in a dinoflagellate. *Proc. Natl. Acad. Sci. USA.* 108:18162–18167.
14. Fogel, M., R. E. Schmitter, and J. W. Hastings. 1972. On the physical identity of scintillons: bioluminescent particles in *Gonyaulax polyedra*. *J. Cell Sci.* 11:305–317.
15. Johnson, C. H., S. Inoué, …, J. W. Hastings. 1985. Compartmentalization of algal bioluminescence: autofluorescence of bioluminescent particles in the dinoflagellate *Gonyaulax* as studied with image-intensified video microscopy and flow cytometry. *J. Cell Biol.* 100:1435–1446.
16. Nicolas, M. T., D. Morse, …, J. W. Hastings. 1991. Colocalization of luciferin binding protein and luciferase to the scintillons of *Gonyaulax polyedra* revealed by double immunolabeling after fast-freeze fixation. *Protoplasma.* 160:159–166.
17. Nawata, T., and T. Sibaoka. 1979. Coupling between action potential and bioluminescence in *Noctiluca* - effects of inorganic ions and pH

in vacuolar sap. *J. Comp. Physiol. A Neuroethol. Sens. Neural Behav. Physiol.* 134:137–149.

18. Wilson, T., and J. W. Hastings. 1998. Bioluminescence. *Annu. Rev. Cell Dev. Biol.* 14:197–230.
19. Schultz, L. W., L. Liu, …, J. W. Hastings. 2005. Crystal structure of a pH-regulated luciferase catalyzing the bioluminescent oxidation of an open tetrapyrrole. *Proc. Natl. Acad. Sci. USA.* 102:1378–1383.
20. Tett, P. B., and M. G. Kelly. 1973. Marine bioluminescence. *Oceanogr. Mar. Biol. Annu. Rev.* 11:89–173.
21. Marcinko, C. L. J., S. C. Painter, …, J. T. Allen. 2013. A review of the measurement and modelling of dinoflagellate bioluminescence. *Prog. Oceanogr.* 109:117–129.
22. Esaias, W. E., and H. C. Curl, Jr. 1972. Effect of dinoflagellate bioluminescence on copepod ingestion rates. *Limnol. Oceanogr.* 17:901–906.
23. White, H. H. 1979. Effects of dinoflagellate bioluminescence on the ingestion rates of herbivorous zooplankton. *J. Exp. Mar. Biol. Ecol.* 36:217–224.
24. Buskey, E., L. Mills, and E. Swift. 1983. The effects of dinoflagellate bioluminescence on the swimming behavior of a marine copepod. *Limnol. Oceanogr.* 28:575–579.
25. Buskey, E. J., and E. Swift. 1985. Behavioral responses of oceanic zooplankton to simulated bioluminescence. *Biol. Bull.* 168:263–275.
26. Buskey, E. J., and E. Swift. 1983. Behavioral responses of the coastal copepod *Acartia hudsonica* (Pinhey) to stimulated dinoflagellate bioluminescence. *J. Exp. Mar. Biol. Ecol.* 72:43–58.
27. Morin, J. G. 1983. Coastal bioluminescence: patterns and functions. *Bull. Mar. Sci.* 33:787–817.
28. Mensinger, A. F., and J. F. Case. 1992. Dinoflagellate luminescence increases susceptibility of zooplankton to teleost predation. *Mar. Biol.* 112:207–210.
29. Abrahams, M. V., and L. D. Townsend. 1993. Bioluminescence in dinoflagellates: a test of the burglar alarm hypothesis. *Ecology.* 74:258–260.
30. Fleisher, K. J., and J. F. Case. 1995. Cephalopod predation facilitated by dinoflagellate luminescence. *Biol. Bull.* 189:263–271.
31. Cusick, K. D., and E. A. Widder. 2013. Intensity differences in bioluminescent dinoflagellate impact foraging efficiency in a nocturnal predator. *Bull. Mar. Sci.* 90:797–811.
32. Latz, M. I., J. C. Nauen, and J. Rohr. 2004. Bioluminescence response of four species of dinoflagellates to fully developed pipe flow. *J. Plankton Res.* 26:1529–1546.
33. von Dassow, P., R. N. Bearon, and M. I. Latz. 2005. Bioluminescent response of the dinoflagellate *Lingulodinium polyedrum* to developing flow: tuning of sensitivity and the role of desensitization in controlling a defensive behavior of a planktonic cell. *Limnol. Oceanogr.* 50:607–619.
34. Hobson, E. S. 1966. Visual orientation and feeding in seals and sea lions. *Nature.* 210:326–327.
35. Rohr, J., M. I. Latz, …, E. Hendricks. 1998. Experimental approaches towards interpreting dolphin-stimulated bioluminescence. *J. Exp. Biol.* 201:1447–1460.
36. Rohr, J., M. Hyman, …, M. I. Latz. 2002. Bioluminescence flow visualization in the ocean: an initial strategy based on laboratory experiments. *Deep-Sea Res.* 49:2009–2033.
37. Latz, M. I., and J. Rohr. 2005. Glowing with the flow: ecology and applications of flow-stimulated bioluminescence. *Optics Photonics News.* 16:40–45.
38. Latz, M. I., J. F. Case, and R. L. Gran. 1994. Excitation of bioluminescence by laminar fluid shear associated with simple Couette flow. *Limnol. Oceanogr.* 39:1424–1439.
39. Latz, M. I., and J. Rohr. 1999. Luminescent response of the red tide dinoflagellate *Lingulodinium polyedrum* to laminar and turbulent flow. *Limnol. Oceanogr.* 44:1423–1435.
40. Müller, D. J., and Y. F. Dufrêne. 2011. Atomic force microscopy: a nanoscopic window on the cell surface. *Trends Cell Biol.* 21:461–469.
41. Dufrêne, Y. F., and A. E. Pelling. 2013. Force nanoscopy of cell mechanics and cell adhesion. *Nanoscale.* 5:4094–4104.
42. Foti, E., C. Faraci, …, G. Bonanno. 2010. On the use of bioluminescence for estimating shear stresses over a rippled seabed. *Meccanica.* 45:881–895.
43. Stokes, M. D., G. B. Deane, …, J. Rohr. 2004. Bioluminescence imaging of wave-induced turbulence. *J. Geophys. Res. Oceans.* 109:C01004.
44. Watanabe, Y., and Y. Tanaka. 2011. Bioluminescence-based imaging technique for pressure measurement in water. *Exp. Fluids.* 51:225–236.
45. Swift, E., and W. R. Taylor. 1967. Bioluminescence and chloroplast movement in the dinoflagellate *Pyrocystis lunula*. *J. Phycol.* 3:77–81.
46. Elbrächter, M., C. Hemleben, and M. Spindler. 1987. On the taxonomy of the lunate *Pyrocystis* species (Dinophyta). *Bot. Mar.* 30:233–242.
47. Stauber, J. L., M. T. Binet, …, M. S. Adams. 2008. Comparison of the Qwiklite algal bioluminescence test with marine algal growth rate inhibition bioassays. *Environ. Toxicol.* 23:617–625.
48. Biggley, W. H., E. Swift, …, H. H. Seliger. 1969. Stimulable and spontaneous bioluminescence in the marine dinoflagellates, *Pyrodinium bahamense, Gonyaulax polyedra*, and *Pyrocystis lunula*. *J. Gen. Physiol.* 54:96–122.
49. Colepicolo, P., T. Roenneberg, …, J. W. Hastings. 1993. Circadian regulation of bioluminescence in the dinoflagellate *Pyrocystis lunula*. *J. Phycol.* 29:173–179.
50. Swift, E., W. H. Biggley, and H. H. Seliger. 1973. Species of oceanic dinoflagellates in the genera *Dissodinium* and *Pyrocystis*: interclonal and interspecific comparisons of the color and photon yield of bioluminescence. *J. Phycol.* 9:420–426.
51. Widder, E. A., M. I. Latz, and J. F. Case. 1983. Marine bioluminescence spectra measured with an optical multichannel detection system. *Biol. Bull.* 165:791–810.
52. Widder, E. A., and J. F. Case. 1981. Two flash forms in the bioluminescent dinoflagellate, *Pyrocystis fusiformis*. *J. Comp. Physiol.* 143:43–52.
53. Latz, M. I., and A. O. Lee. 1995. Spontaneous and stimulated bioluminescence in the dinoflagellate, *Ceratocorys horrida* (Peridiniales). *J. Phycol.* 31:120–132.
54. Livolant, F. 1982. Dinoflagellate trichocyst ultrastructure. 1. The shaft. *Biol. Cell.* 43:201–210.
55. Livolant, F. 1982. Dinoflagellate trichocyst ultrastructure. 2. Existence of a sheath. *Biol. Cell.* 43:211–216.
56. Seo, K. S., and L. Fritz. 2002. Ultrastructure of vegetative cysts of *Pyrocystis* (Dinophyta), with special reference to PAS bodies and trichocysts. *Phycologia.* 41:10–14.
57. Latz, M. I., M. Bovard, …, A. Groisman. 2008. Bioluminescent response of individual dinoflagellate cells to hydrodynamic stress measured with millisecond resolution in a microfluidic device. *J. Exp. Biol.* 211:2865–2875.
58. Buskey, E. J., S. Strom, and C. Coulter. 1992. Bioluminescence of heterotrophic dinoflagellates from Texas coastal waters. *J. Exp. Mar. Biol. Ecol.* 159:37–49.
59. Sullivan, J. M., and E. Swift. 1995. Photoenhancement of bioluminescence capacity in natural and laboratory populations of the autotrophic dinoflagellate *Ceratium fusus* (Ehrenb.) Dujardin. *J. Geophys. Res.* 100:6565–6574.
60. Swift, E., and V. Meunier. 1976. Effects of light intensity on division rate, stimulable bioluminescence and cell size of the oceanic dinoflagellates *Dissodinium lunula, Pyrocystis fusiformis* and *P. noctiluca*. *J. Phycol.* 12:14–22.
61. Skalak, T. C., and R. J. Price. 1996. The role of mechanical stresses in microvascular remodeling. *Microcirculation.* 3:143–165.
62. Cherry, R. S., and E. T. Papoutsakis. 1990. Understanding and controlling fluid-mechanical injury of animal cells in bioreactors. *Animal Cell Biotechnology.* 4:71–121.

63. Huang, H., R. D. Kamm, and R. T. Lee. 2004. Cell mechanics and mechanotransduction: pathways, probes, and physiology. *Am. J. Physiol. Cell Physiol.* 287:C1–C11.

64. Ingber, D. E. 2006. Cellular mechanotransduction: putting all the pieces together again. *FASEB J.* 20:811–827.

65. Davies, P. F. 1995. Flow-mediated endothelial mechanotransduction. *Physiol. Rev.* 75:519–560.

66. Hamill, O. P., and B. Martinac. 2001. Molecular basis of mechanotransduction in living cells. *Physiol. Rev.* 81:685–740.

67. Na, S., O. Collin, …, N. Wang. 2008. Rapid signal transduction in living cells is a unique feature of mechanotransduction. *Proc. Natl. Acad. Sci. USA.* 105:6626–6631.

68. Charras, G. T., and M. A. Horton. 2002. Determination of cellular strains by combined atomic force microscopy and finite element modeling. *Biophys. J.* 83:858–879.

69. Latz, M. I., A. R. Juhl, …, J. Rohr. 2004. Hydrodynamic stimulation of dinoflagellate bioluminescence: a computational and experimental study. *J. Exp. Biol.* 207:1941–1951.

70. Ohashi, T., Y. Ishii, …, M. Sato. 2002. Experimental and numerical analyses of local mechanical properties measured by atomic force microscopy for sheared endothelial cells. *Biomed. Mater. Eng.* 12:319–327.

71. Kuznetsova, T. G., M. N. Starodubtseva, …, R. I. Zhdanov. 2007. Atomic force microscopy probing of cell elasticity. *Micron.* 38:824–833.

72. Zhang, X., X. Liu, …, H. K. Pak. 2008. Real-time observations of mechanical stimulus-induced enhancements of mechanical properties in osteoblast cells. *Ultramicroscopy.* 108:1338–1341.

73. Radmacher, M. 2002. Measuring the elastic properties of living cells by the atomic force microscope. *In* Methods in Cell Biology. Academic Press, San Diego, CA, pp. 67–90.

74. Touhami, A., B. Nysten, and Y. F. Dufrene. 2003. Nanoscale mapping of the elasticity of microbial cells by atomic force microscopy. *Langmuir.* 19:4539–4543.

75. Francius, G., B. Tesson, …, Y. F. Dufrêne. 2008. Nanostructure and nanomechanics of live *Phaeodactylum tricornutum* morphotypes. *Environ. Microbiol.* 10:1344–1356.

76. Higgins, M. J., J. E. Sader, …, R. Wetherbee. 2003. Probing the surface of living diatoms with atomic force microscopy: the nanostructure and nanomechanical properties of the mucilage layer. *J. Phycol.* 39:722–734.

77. Milani, P., M. Gholamirad, …, O. Hamant. 2011. In vivo analysis of local wall stiffness at the shoot apical meristem in *Arabidopsis* using atomic force microscopy. *Plant J.* 67:1116–1123.

78. Peaucelle, A., S. A. Braybrook, L. Le Guillou, …, H. Hofte. 2011. Pectin-induced changes in cell wall mechanics underlie organ initiation in *Arabidopsis*. *Current Biol.* 21:1720–1726.

79. Swift, E., and C. C. Remsen. 1970. The cell wall of *Pyrocystis* spp. (Dinococcales). *J. Phycol.* 6:79–86.

80. Seo, K. S., and L. Fritz. 2000. Cell-wall morphology correlated with vertical migration in the non-motile marine dinoflagellate *Pyrocystis noctiluca*. *Mar. Biol.* 137:589–594.

81. Heimann, K., P. L. Klerks, and K. H. Hasenstein. 2009. Involvement of actin and microtubules in regulation of bioluminescence and translocation of chloroplasts in the dinoflagellate *Pyrocystis lunula*. *Bot. Mar.* 52:170–177.

82. McDougall, C. 2002. Bioluminescence and the actin cytoskeleton in the dinoflagellate *Pyrocystis fusiformis*: an examination of organelle transport and mechanotransduction. PhD thesis. University of California Santa Barbara.

83. Seo, K. S., and L. Fritz. 2000. Cell ultrastructural changes correlate with circadian rhythms in *Pyrocystis lunula* (Pyrrophyta). *J. Phycol.* 36:351–358.

84. Sato, K., T. Adachi, …, Y. Tomita. 2007. Measurement of local strain on cell membrane at initiation point of calcium signaling response to applied mechanical stimulus in osteoblastic cells. *J. Biomech.* 40:1246–1255.

85. Frey, J. W., E. E. Farley, …, T. A. Hornberger. 2009. Evidence that mechanosensors with distinct biomechanical properties allow for specificity in mechanotransduction. *Biophys. J.* 97:347–356.

86. Eckert, R., and T. Sibaoka. 1968. The flash-triggering action potential of the luminescent dinoflagellate *Noctiluca*. *J. Gen. Physiol.* 52:258–282.

87. Maldonado, E. M., and M. I. Latz. 2007. Shear-stress dependence of dinoflagellate bioluminescence. *Biol. Bull.* 212:242–249.

88. Frangos, J. 1993. Physical Forces and the Mammalian Cell. Academic Press, San Diego, CA.

89. Ballermann, B. J., and M. J. Ott. 1995. Adhesion and differentiation of endothelial cells by exposure to chronic shear stress: a vascular graft model. *Blood Purif.* 13:125–134.